



**HAL**  
open science

# Original Design Procedure For Self-Reconfigurable Low Noise Figure and High RF Input Power Overdrive LNAs: Application To X-Band GaN MMICs

Jean-Guy Tartarin, Bastien Pinault, Damien Saugnon

## ► To cite this version:

Jean-Guy Tartarin, Bastien Pinault, Damien Saugnon. Original Design Procedure For Self-Reconfigurable Low Noise Figure and High RF Input Power Overdrive LNAs: Application To X-Band GaN MMICs. IEEE International Conference on Noise and Fluctuations, Chistoforos Theodorou, Oct 2023, Grenoble, France. 10.1109/ICNF57520.2023.10472740 . hal-04440655

**HAL Id: hal-04440655**

**<https://hal.science/hal-04440655>**

Submitted on 6 Feb 2024

**HAL** is a multi-disciplinary open access archive for the deposit and dissemination of scientific research documents, whether they are published or not. The documents may come from teaching and research institutions in France or abroad, or from public or private research centers.

L'archive ouverte pluridisciplinaire **HAL**, est destinée au dépôt et à la diffusion de documents scientifiques de niveau recherche, publiés ou non, émanant des établissements d'enseignement et de recherche français ou étrangers, des laboratoires publics ou privés.



Distributed under a Creative Commons Attribution - NonCommercial 4.0 International License

# Original Design Procedure For Self-Reconfigurable Low Noise Figure and High RF Input Power Overdrive LNAs: Application To X-Band GaN MMICs

Jean-Guy Tartarin  
LAAS-CNRS and University of  
Toulouse  
Toulouse, France  
[tartarin@laas.fr](mailto:tartarin@laas.fr)

Bastien Pinault  
LAAS-CNRS and University of  
Toulouse  
Toulouse, France  
[bpinault@laas.fr](mailto:bpinault@laas.fr)

Damien Saugnon  
LAAS-CNRS  
Toulouse, France  
[dsaugnon@laas.fr](mailto:dsaugnon@laas.fr)

**Abstract**—This article proposes an original method for designing Low Noise Amplifiers on wide-bandgap RF technologies. These LNAs are able to withstand high electromagnetic signals, like those used in electronic warfare, while providing high detectivity. The study presents the original design procedure of a single-stage LNA and a two-stage LNA based on the same strategy. These self-reconfigurable LNAs make it possible to switch from a high detectivity mode (low NF) to a high linearity mode (high input compression mode  $IP_{1dB}$ ). This design strategy is compared to a robust LNA design, which uses a larger transistor size for improved linearity at the cost of a slight NF degradation. RF step-stress results has been performed up to 30 dBm at the input of the amplifier without any destruction, and providing stable S-parameters and noise figure.

**Keywords**—GaN, MMIC LNA, robust receiver, self-reconfigurable LNA, highly linear, low NF, RF step stress.

## I. INTRODUCTION

While LNAs based on CMOS technology suffer from a reduction of the supply voltage as a consequence of the reduction of the channel length (scaling of the CMOS voltage, i.e. [1]), and therefore a reduction of the maximum RF overdrive in linear mode or before destruction, wide bandgap technologies, such as Nitride technologies, open the way to the design of new amplifier architectures, mainly for power amplification. In the case of Low Noise Amplifiers (LNA), GaN High Electron Mobility Transistor (HEMT) allows both good detectivity (low Noise Figure at 50  $\Omega$  input matching -  $NF_{50}$ ) and improved robustness against electromagnetic (EM) waves for applications in harsh environment. In addition, these technologies can withstand high temperatures and can be placed at a very close distance from the antenna. With the increasing complexity related to the integration of multiple TxRx modules in Active Electronically Scanned Array systems, the separation of the protection device (radar burn-trough) and the LNA represents a limitation in the available space, while the necessary use of the limiter (protection system) degrades the overall detectivity by at least 1 dB at 10 GHz. The development of MMIC LNAs capable of handling high RF powers paves the way to a new generation of receivers, also taking into account the limitation of space once these RF frontends are packaged. While designers have started designing robust LNA circuits based on Nitride technologies over the past decade, few different

strategies have been proposed in the literature [2][3]. In these articles, the maximum RF power that can be applied to the input of the LNA is taken into account at the end of the design cycle (conventional approach), or at the beginning of this procedure when choosing the transistor [4]: an interesting solution first proposed by M. Rudolph uses a larger size HEMT to achieve better linearity at the cost of a slightly degraded  $NF_{50}$  compared to the classical method. For radar or for satellite telecommunication systems, high-power microwave effect degrades the Bit Error Rate (BER) [5], and ultimately can also damage the receiver system.

In the second section, the proposed design procedure is summarized and compared to the conventional design methodology. The third section presents the measured performances of scattering parameters,  $NF_{50}$  and input power compression  $IP_{1dB}$  for the single-stage LNAs under study: our approach is compared to that developed in [4]. Then RF step-stress results are proposed for the single-stage LNAs, extended to a two-stage LNA using our design strategy. A conclusion summarizes this work, with a comparison with state-of-the-art LNAs considering  $NF_{50}$  versus  $IP_{1dB}$  for Nitride technologies.

## II. DESIGN PROCEDURE FOR (SELF)RECONFIGURABLE LNA: LOW $NF_{50}$ AND HIGH $IP_{1dB}$

### A. General considerations of narrow bandgap technologies versus wide bandgap technologies

For every RF circuit design, it all starts at the transistor level: the selection of the size and bias of the HEMT is crucial for the final performance of the circuit (and we should add also for the evaluation of its lifetime, when considering the stresses it is subjected to and other SOA rules!). In this article, only general considerations are given for the design of a GaN LNA. Of course, from a MMIC technology provider to another one, the recipe should be managed in a different way and this is why only the principal advices are given. First, as we deal with an amplifier function, the transconductance gain  $g_m$  is primordial. Moreover  $g_m$  also impacts detectivity (or whatever noise model is used, the four noise parameters!). Fig. 1 compares the static transfer characteristics with the transconductance gain of a narrow bandgap III-V technology (ED02AH) and of a widebandgap N-V technology (D01GH) from OMMIC. It is obvious that the maximum  $g_m$  peaks near the threshold voltage

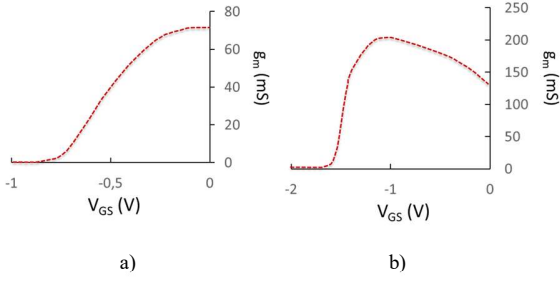


Fig. 1. Static simulation of the transconductance profile versus  $V_{GS}$  for a narrow bandgap technology -a, and for a wide bandgap technology -b (resp. OMMIC ED02AH and D01GH).

for the GaN HEMT, while  $g_m$  decreases drastically for the III-V HEMT close to the pinchoff. Moreover,  $g_m$  is 10 times higher than for III-V HEMT at the optimum quiescent point for low noise applications (around  $I_{DSS}/3$  for III-V,  $I_{DSS}/5$  for N-V). Thus, the design of the two LNAs cannot be driven in the same way. Next, we consider the GaN technology. Whatever the transistor's noise model, the transconductance gain  $g_m$ , the resistance of the gate and of the source ( $R_S$ ,  $R_G$ ) or drain-source ( $R_{DS}$ ) are the main parameters that play a role in the noise temperature or in the noise figure expression. Popiezalski's empirical model for the minimum achievable noise temperature  $T_{min}$  [6] is calculated by highlighting  $g_m$ , and finally expressed according to (1), in an expression very close to those that can be found in other related models. Also (2) proposes the minimum noise factor  $F_{min}$  based on Fukui's model [7]. This model, although originally developed for MESFETs, is still relevant for HEMT devices providing higher  $g_m$  and a reduction of  $R_S$  and  $R_G$  resistances.  $K_f$  coefficient is related to the channel material and gate length. Whatever these models,  $g_m$  plays a role in the noise equations, as well as the resistances  $R_G$  and  $R_S$  and  $C_{GS}$  capacitor. This determines the transistor selection in relation with electrical parameters (DC plots and S-parameters).

$$T_{min} = \frac{4\pi C_{GS} f}{g_m} \sqrt{\frac{R_i T_g T_d}{R_{DS}} + \left(\frac{2\pi C_{GS} f}{g_m} \frac{R_i T_d}{R_{DS}}\right)^2} + \left(\frac{2\pi C_{GS} f}{g_m}\right)^2 \frac{2R_i T_d}{R_{DS}} \quad (1)$$

$$F_{min} = 1 + K_f 2\pi C_{GS} f \sqrt{\frac{(R_G + R_S)}{g_m}} \quad (2)$$

Not shown in the direct expression of (1) and (2), the drain current  $I_{DS}$  generates noise, as can be seen in [8] from Cappy, and rewritten in (3) as a function of  $g_m$ .  $I_{DS}$  has to be kept at a lower value, but still with elevated  $g_m$ . This is one of the great interest of GaN technologies regarding the  $g_m(V_{GS})$  profile near the pinchoff zone where  $g_m$  is maximum. Fig. 2 plots  $g_m$  versus  $I_{DS}$ , and the inflexion zone where  $g_m$  decreases for the lower  $I_{DS}$  quiescent points represents the optimum biasing condition to use. The quick decreasing of  $g_m$  on the lower  $I_{DS}$  zone must be avoided for model dispersion (process variations from DOE), and reliability purposes (sensitivity to positive or negative bias temperature instabilities PBTI/NBTI).

$$F_{min} = 1 + 2 \sqrt{\frac{V_i}{E_{CL}}} \frac{2\pi C_{GS} f}{\sqrt{g_m}} \sqrt{(R_G + R_S)} \quad (3)$$

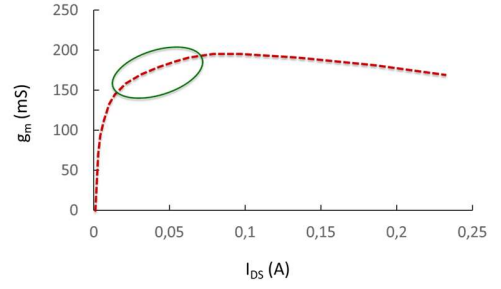


Fig. 2. Static simulation of the transconductance  $g_m$  versus  $I_{DS}$  for a 6x40 gate width HEMT biased at  $V_{DS} = 5$  V (OMMIC D01GH). In green circle is represented the optimum biasing zone for maximum gain and low noise.

Finally, for circuit designers, the four noise parameters to consider yield the noise factor  $F$  as formalized in (4):

$$F = F_{min} + \frac{R_n}{G_S} |Y_S - Y_{opt}|^2 \quad (4)$$

Where  $R_n$  is the equivalent noise resistance,  $Y_S = G_S + jB_S$  the source admittance and  $Y_{opt}$  the optimum noise admittance. Next noise figures are used, expressed in decibel as  $NF_{min} = 10 \cdot \log(F_{min})$ .

#### B. Design fundamentals versus new design flow

Below we summarize the LNA design steps by the conventional strategy, and by the approach adopted in this work. The gate length for all designs is 100 nm. For the conventional design flow, the first parameters to consider concern the noise and small-signal characteristics. Linearity and other considerations are taken into account only at the end, and they are usually satisfied in a multi-stage topology. The proposed strategy also integrates linearity at the very beginning of the LNA design process.

##### Conventional design flow : best $NF_{50}$

###### ■ Transistor selection (size/bias):

- Minimize the noise of the amplifier  $NF_{50}$  regarding the source impedance matching (admittance  $Y_S$ ) to approach  $NF_{min}$ .
- According to the frequency band, the noise resistance should be carefully considered.
- Use inductive serial feedback to meet small-signal and noise matching at the input.

###### ■ Design fundamentals:

- Design the lumped/real elements (design kit) matching network at the input (source) and output (load) of the LNA: evaluation of passives (inductor/capacitor quality factor, line losses). Also considering the DOE (technological dispersion).
- DC power management.  $P_{DC}$  is usually low for LNA (drain current reduction is mandatory, still keeping  $g_m$  high), and then appears the conflict between NF and IIP3.

once the MMIC achieved, evaluate the maximum RF overdrive before destruction.

These fundamental rules can be used to design the rugged LNAs as in [4], but considering the  $IP_{1dB}$  at the earlier step, as for  $NF_{min}$ . Improving  $IP_{1dB}$  comes with the price of

compromising noise and linearity. Next, the design flow is completed with linearity considerations.

### Complete design flow : best $NF_{50}$ and high $IP_{1dB}$

#### ■ Transistor selection.

-A mapping is realized on the sizing/biasing of the HEMTs at the center frequency of 10 GHz as proposed in Fig. 3, considering  $NF_{min}$  and  $IP_{1dB}$ . The objective is to find a device capable of being tuned from the best  $NF_{min}$  to the highest  $IP_{1dB}$  by changing the only tunable parameter of the MMIC process: the quiescent point. The  $g_m$  is also checked to be at the same value when changing the DC bias to keep the small signal gain  $S_{21}$  stable when switching from high detectivity mode to high linearity mode (and vice versa). For this study, a  $6 \times 40 \mu m$  gate width transistor has been selected operating at  $(V_{DS}, I_{DS})$  of (5V, 50 mA) in high detectivity mode ( $NF_{min}=0.44$  dB,  $IP_{1dB}=8$  dBm) and  $(V_{DS}, I_{DS})$  of (10 V, 120 mA) in high linearity mode ( $NF_{min}=0.87$  dB,  $IP_{1dB}=15$  dBm). The optimization on  $IP_{1dB}$  is achieved by increasing  $P_{DC}=V_{DS} \cdot I_{DS}$ ; increasing  $V_{DS}$  and keeping  $I_{DS}$  low enough allows a degradation of  $NF_{min}$  by only 0.4 dB between the two modes (cf. Fig. 1 and equ. 3). This is relatively small considering the 1 dB degradation of  $NF_{50}$  associated to the presence of a limiter, in conventional receivers.

-Evaluate the trap effects (by model if available, or by considering lag metrics on output characteristics) according to the selection of DC-biasing paths in the output characteristics. All other consideration is following the conventional design flow.

#### ■ Design fundamentals:

-The first steps are very close to the conventional flow, but the input/output reflexion coefficient should be constant to allow a good matching whatever the operating mode of the LNA. Moreover, the inconditionnal stability should be efficient when changing the DC bias between these operating modes (and also considering the critical DC-path between those quiescent points). Special care is given to the robustness of the MMIC stability when changing the DC bias. Iterations should be done between topology and device selection if stability cannot be satisfied within DC-paths. The two-stage design accounts for all the noise and linearity budget from the first stage, and the biasing is performed on each of the two stages for a maximum of dynamic in  $IP_{1dB}$ .

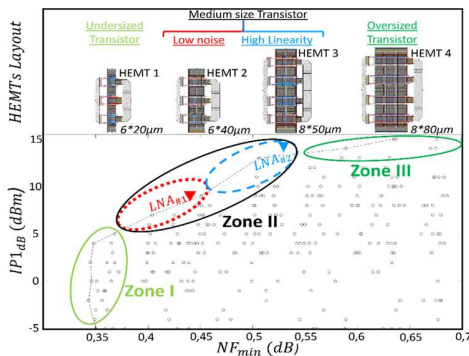


Fig. 3. Device biasing and sizing selection for Low Noise or high compression  $IP_{1dB}$  purposes ( $NF_{min}$  versus  $IP_{1dB}$  @10 GHz). Sizing is for number of gate fingers and gate individual width respectively ranging between [2;4;6;8] and [20  $\mu m$  to 100  $\mu m$  by step of 20  $\mu m$ ], while biasing on  $V_{GS}$  and  $V_{DS}$  respectively range between [-1,7 V to 0 V by step of 0.2 V] and [3 V;5 V;8 V;12 V;20 V]. The number of random sizing/DC biasing combinations is 1000.

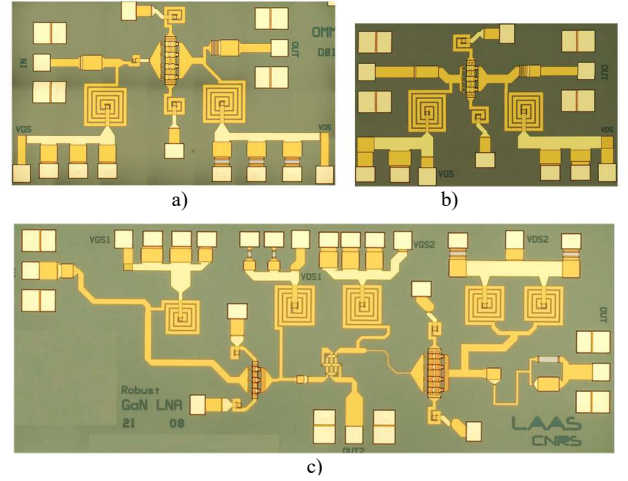
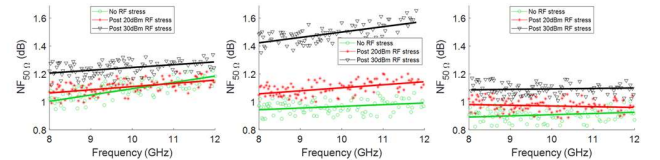


Fig. 4. Pictures of the a) single-stage rugged LNA (HEMT  $8 \times 50 \mu m$  biased at  $V_{DS}=12$  V and  $I_{DS}=48$  mA) and b) single-stage self-reconfigurable LNA ( $4 \times 60 \mu m$  biased at  $V_{DS}=5/10$  V and  $I_{DS}=50/120$  mA), and of the c) two-stage reconfigurable LNA. All LNAs operate in the 8 GHz - 12 GHz frequency band. Scales between circuits are respected.

-The maximum RF power rating is evaluated with the non-linear model and the SOA.

### III. MEASUREMENT OF THE SELF-RECONFIGURABLE LNA AND OF THE RUGGED LNA

Two single-stage LNAs have been designed and measured; the rugged LNA featuring a large size HEMT ( $8 \times 50 \mu m$ ), and the self-reconfigurable LNA featuring a small size HEMT ( $6 \times 40 \mu m$ ) (resp. Fig. 3.a and Fig. 3.b). Special care has been given to the small-signal gain for self-reconfigurable LNAs, for which a constant gain is expected whatever the configuration. One two-stage LNA has been designed and measured [9], also self-reconfigurable but with a higher small-signal gain ( $>20$  dB). All circuits are input/output matched with return loss lower than -10 dB over the 8 GHz - 12 GHz bandwidth. RF step-stresses have been performed up to 35 dBm at the input of the LNAs. No degradation on electrical and noise parameters occurs up to  $P_{in}=30$  dBm [10]. Performances of 1-stage and 2-stage LNAs are summarized in Table I. Noise Figure measurements are performed with the PNA-X series 5244B from Keysight, option 029 (low noise measurement) for accurate measurement. Fig. 5 provides  $NF_{50}$  measurements over 8GHz-12GHz bandwidth for the LNAs under test.



a) Rugged LNA & new strategy of LNA b) LN mode c) HL mode

Fig. 5. X-band noise figure measurements for the two 1-stage LNAs under test. a)  $NF_{50}$  for the rugged design.  $NF_{50}$  for the reconfigurable LNA under Low Noise operating mode b) and under High Linearity operating mode c). Measurements are performed at initial state t0 (green plots), and after different RF-step stresses: sequence #1 is after the  $P_{in}=20$  dBm step stress (red plots) and sequence #2 is after the  $P_{in}=30$  dBm step stress (black plots). Fatal failure occurs at  $P_{in}=35$  dBm for all LNAs under test.

TABLE I. ELECTRICAL AND NOISE PERFORMANCE OF THE X-BAND MMIC LNAs

Type of LNA	Electrical and Noise performance between 8 GHz and 12 GHz				
	NF50 dB	S <sub>21</sub> dB	S <sub>11</sub> /S <sub>22</sub> dB	IP <sub>1dB</sub> dBm no damage @ 10GHz	Max. RF input power dBm @ 10GHz
1-stage rugged LNA	< 1.3	> 9	< -11 / < -14	+20	35
1-stage self-reconfigurable LNA (high detectivity / high linearity mode)	< 0.95 < 1.4	> 10 > 10	< -10 / < -11 < -10 / < -11	+4 +14	35 35
2-stage self-reconfigurable LNA (high detectivity / high linearity mode)	< 1.6 < 2.1	> 19 > 19	< -10 / < -11 < -10 / < -11	-5 +5	N.A

The LNA circuits support powers up to 20 dBm without degradation. A slight degradation occurs on NF50 for input power of 30 dBm (+0.5 dB and +0.2 dB / +0.1 dB respectively for 1-stage Rugged LNA and 1-stage reconfigurable LNA under Low Noise mode / High Linearity mode). The fatal failure appears at 35 dBm, concomitant with a rapid increase in the leakage current (all circuits show 10 mA gate leakage current at 30 dBm RF input power). Regardless of the design or bias strategy, the fatal failure appears to be related to the leakage current limitation of the Schottky gate, imposed by the technology-related operational safety zone, and device size or DC bias is not a first-order consideration. Fig. 6 depicts the PCB self-reconfiguring system with the power to DC converter and the MMIC chip (Fig. 6.a), as well as the synoptic of the whole system (Fig. 6.b). A full MMIC version has also been

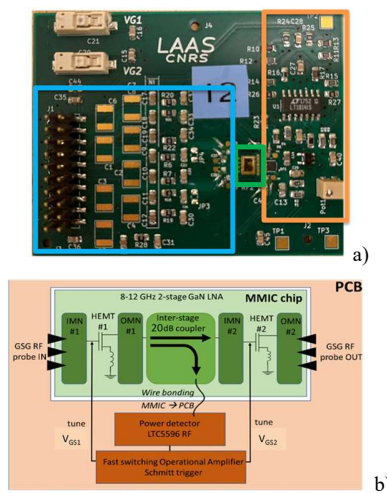


Fig. 6. System with the MMIC chip reported on a PCB (a): picture of the MMIC chip in green rectangle, biasing circuit with power detector and Schmitt trigger in orange rectangle and medium to low frequency stability circuits in blue rectangle. The synoptic of the PCB and MMIC chips given in (b) for the self-control of the biasing strategy between High-detectivity mode and High-linearity mode for the 2-stage LNA. The output pad of the single-stage LNAs or at the lange coupler situated between the two stages of the 2-stage LNA (MMIC) is connected to the RF to DC converter (power detector) by wire bonding. Then the DC signal is applied to a trigger of Schmitt. The hysteresis can be adjusted to select the two RF power thresholds (from high-detectivity mode to high-linearity protection mode, or from high-linearity to high-detectivity nominal mode).

successfully designed, with an integration as low as 2mm<sup>2</sup> chip. This fully integrated proof of concept should be of interest for robust self-reconfigurable receivers in AESA systems.

#### IV. CONCLUSIONS

This study compares different design versions of wide bandgap GaN MMIC LNAs operating in X-band. The conventional approach (high detectivity mode configuration) and the rugged design are compared to our self-reconfigurable design that offers flexibility between noise figure and input power at 1 dB compression. It is demonstrated that the receiver can adjust from a high detectivity mode to a protection mode by increasing IP<sub>1dB</sub> by 10 dB (according to the detection of a critical EM signal level). One critical point during the design process of these GaN amplifiers concerns the unconditional stability to be achieved. We demonstrate that our self-reconfigurable LNA can operate safely on various DC quiescent points under CW RF signals. Also the pulsed biasing has been validated for all of the measured LNAs with rise and fall time of less than 30 μs. This makes the LNAs available for CW and for pulsed applications.

#### ACKNOWLEDGMENT

This work was supported by the LAAS-CNRS PROOF platform, partly financed by the Occitanie region.

#### REFERENCES

- [1] M. White and Y. Chen, "Scaled CMOS technology reliability users guide," JPL Publ., pp. 08-14, 2008, [Online]. Available: [http://parts.jpl.nasa.gov/docs/NEPP07/NEPP\\_07\\_Scaled\\_CMOS\\_Technology\\_Reliability\\_Users\\_Guide\\_\(Released\\_CL#08-0939\).pdf](http://parts.jpl.nasa.gov/docs/NEPP07/NEPP_07_Scaled_CMOS_Technology_Reliability_Users_Guide_(Released_CL#08-0939).pdf).
- [2] S. D. Nsele *et al.*, « Ka-band low noise amplifiers based on InAlN/GaN technologies », in *2015 International Conference on Noise and Fluctuations (ICNF)*, Xian, China, juin 2015, p. 1-4. doi: 10.1109/ICNF.2015.7288577.
- [3] S. Zafar *et al.*, « GaN based LNA MMICs for X-Band Applications », in *2020 17th International Bhurban Conference on Applied Sciences and Technology (IBCANT)*, Islamabad, Pakistan, janv. 2020, p. 699-702. doi: 10.1109/IBCANT47879.2020.9044569.
- [4] M. Rudolph *et al.*, « Highly robust X-band LNA with extremely short recovery time », in *2009 IEEE MTT-S International Microwave Symposium Digest*, Boston, MA, USA, juin 2009, p. 781-784. doi: 10.1109/MWSYM.2009.5165813.
- [5] F. Lu, Z. Qiu, X. Gu, B. Zhang and Z. Xin, « Efficiency Analysis of High Power Microwaves Jamming Digital Communication System » *2020 23rd International Microwave and Radar Conference (MIKON)*, Warsaw, Poland, 2020, pp. 136-139, doi: 10.23919/MIKON48703.2020.9253907.
- [6] M. W. Pospieszalski, « Modeling of noise parameters of MESFETs and MODFETs and their frequency and temperature dependence », *IEEE Transactions on Microwave Theory and Techniques*, vol. 37, no. 9, pp. 1340-1350, Sept. 1989, doi: 10.1109/22.32217.
- [7] H. Fukuy, « Design of Microwave GaAs MESFETs for Broadband, Low-Noise Amplifiers », *IEEE Transactions on Microwave Theory and Techniques*, vol. MTT-27, pp. 643-650, July 1979.
- [8] A. Cappy, « Noise modeling and measurement techniques (HEMTs) », *IEEE Transactions on Microwave Theory and Techniques* 36.1 (1988): 1-10.
- [9] B. Pinault *et al.*, « A Reconfigurable Highly Linear and Robust X-Band GaN LNA », 1<sup>st</sup> Space Microwave Week 2023, European Space Agency (ESA), May 2023, Noordwijk, Netherlands. hal-04142799. Unpublished
- [10] B. Pinault, J.G. Tartarin, D. Saugnon, R. Leblanc, « Impact of RF stress on different topologies of 100 nm X-band robust GaN LNA » *Microelectronics Reliability Journal*, Elsevier, 6 p., October 2023. <https://doi.org/10.1016/j.microrel.2023.11512>.